Binding of Phosphate with a Simple Hexaaza Polyammonium Macrocycle

Olga A. Gerasimchuk, Susan Mason, José M. Llinares, Maoping Song, Nathaniel W. Alcock,*,† and Kristin Bowman-James*

Department of Chemistry, University of Kansas, Lawrence, Kansas 66045, and Department of Chemistry, University of Warwick, Coventry CV4 7AL, Great Britain

Received September 16, 1999

A mixture of dihydrogen phosphate and phosphoric acid has been crystallized with a hexaprotonated 26-membered polyammonium macrocycle, 1,4,7,14,17,20-hexaazacyclohexacosane, as the counterion. The complex crystallizes in the monoclinic space group $P2_1/c$ with unit cell parameters of $a = 10.006(2)$ Å, $b = 12.525(1)$ Å, $c = 19.210(2)$ Å, $\beta = 102.91(1)°$, and $V = 2346.6(5)$ Å^3. The hexaprotonated macrocycle is located on a crystallographic center of inversion and is surrounded by eight phosphate anions. Six of the phosphates are dihydrogen phosphates ($H_2PO_4^-$), and the other two are neutral phosphoric acid molecules. Intricate hydrogen-bonding networks, involving the anionic and neutral phosphates and the protonated macrocycle, dominate the crystal lattice. Potentiometric studies using NaCl as the supporting electrolyte indicate high formation constants for the triprotonated macrocycle, H_3L^{3+}, with PO_4^{3-} at pH ∼9.5 ($\log K = 4.55(4)$), for the tetraprotonated macrocycle, H_4L^{4+}, with monohydrogen phosphate, HPO_4^{2-}, at pH ∼8.0 ($\log K = 6.01(3)$), and for ditopic complexes with H_5L^{5+} and H_6L^{6+} and dihydrogen phosphate, $H_2PO_4^-$, at pH ∼4.0 ($\log K = 6.16(6)$) and pH ∼2.5 ($\log K = 6.44(5)$), respectively. The ditopic behavior in the simple polyazamacrocycle receptor is a somewhat unusual occurrence, as is the finding of phosphoric acid species in the crystal structure.

Introduction

The field of anion-coordination chemistry has surged over the last two decades.[1−12] Interest in the influence of simple oxo anions such as phosphates and nitrates on the environment has provided a major impetus to this area. For a number of years, we have explored the design and synthesis of polyammonium macrocycles both as receptors for nucleotides and as catalysts for phosphoryl transfer reactions.[2,13−20] More recently, our focus has shifted to investigating these receptors as hosts for simpler anions. Thus, in an endeavor to design molecules capable of the selective recognition of different oxo anions, we have embarked on an exploration of how structural and topological effects influence the selectivity of macrocyclic receptors for specific anions. In the initial phase of this study, we isolated and characterized a number of macrocyclic complexes with nitrate ions.[21−23] Phosphates are also of widespread use in our culture, for example, as preservatives in foods and as additives to detergents. Consequently, these anions have a major impact on the environment as well, and finding selective receptors for them is, likewise, a valuable undertaking.

In our ongoing studies, we isolated a phosphate-containing salt of a hexaaza macrocycle, 1,4,7,14,17,20-hexaazacyclohexacosane, [26]aneN_6C_6 (**1**). We were surprised to discover that

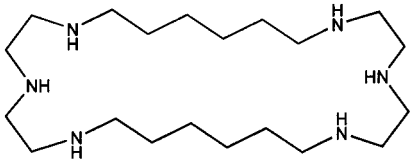

1, [26]aneN_6C_6

the crystal structure indicated eight phosphate species, because the macrocycle contains only six amines capable of protonation.

† University of Warwick.

(1) *Supramolecular Chemistry of Anions*; Bianchi, A., Bowman-James, K., García-España, E., Eds.; Wiley−VCH: New York, 1997.
(2) Mertes, M. P.; Mertes, K. B. *Acc. Chem. Res.* **1990**, *23*, 413−418.
(3) Beer, P. D.; Wheeler, J. W.; Moore, C. *Supramolecular Chemistry*; Balzani, V., De Cola, L., Eds.; Kluwer Academic Publishers: The Netherlands, 1992; pp 105−118.
(4) Katz, H. E. In *Inclusion Compounds*; Atwood, J. L., Davies, J. E. D., MacNichol, D. D., Eds.; Oxford University Press: Oxford, 1991; pp 391−405.
(5) Dietrich, B.; Guilhem, J.; Lehn, J.-M.; Pascard, C.; Sonveaux, E. *Helv. Chim. Acta* **1984**, *67*, 91−104.
(6) Dietrich, B. *Pure Appl. Chem.* **1993**, *65*, 1457−1464.
(7) Izatt, R. M.; Pawlak, K.; Bradshaw, J. S.; Bruening, R. L. *Chem. Rev.* **1991**, *91*, 1721−2085.
(8) Vögtle, F.; Sieger, H.; Müller, W. M. *Top. Curr. Chem.* **1981**, *98*, 107−161.
(9) Crompton, T. R. *Determination of Anions*; Springer: New York, **1996**.
(10) Kimura, E. *Top. Curr. Chem.* **1985**, *128*, 113−141.
(11) Sessler, J. L.; Cyr, M.; Furuta, H.; Kral, V.; Mody, T.; Morishma, T.; Shionaya, M.; Weghorn, S. *Pure Appl. Chem.* **1993**, *65*, 393−398.
(12) Beer, P. D.; Smith, D. K. *Prog. Inorg. Chem.* **1997**, *46*, 1−96.
(13) Yohannes, P. G.; Mertes, M. P.; Mertes, K. B. *J. Am. Chem. Soc.* **1985**, *107*, 8288−8289.
(14) Hosseini, M. W.; Lehn, J.-M.; Maggiora, L.; Mertes, K. B.; Mertes, M. P. *J. Am. Chem. Soc.* **1987**, *109*, 537−544.
(15) Yohannes, P. G.; Mertes, M. P.; Mertes, K. B. *Inorg. Chem.* **1987**, *26*, 1751−1755.
(16) Jahansouz, H.; Jiang, Z.; Himes, R. H.; Mertes, M. P.; Mertes, K. B. *J. Am. Chem. Soc.* **1989**, *111*, 1409−1413.
(17) Hosseini, M. W.; Lehn, J.-M.; Jones, K. C.; Plute, K. E.; Mertes, K. B.; Mertes, M. P. *J. Am. Chem. Soc.* **1989**, *111*, 6330−6335.
(18) Jiang, Z.; Chalabi, P.; Mertes, K. B.; Jahansouz, H.; Himes, R. H.; Mertes, M. P. *Bioorg. Chem.* **1989**, *17*, 313−319.
(19) Qian, L.; Sun, Z.; Gao, J.; Movassagh, B.; Morales, L.; Mertes, K. B. *J. Coord. Chem.* **1991**, *23*, 155−172.
(20) Bencini, A.; Bianchi, A.; Garcia-Espana, E.; Scott, E. C.; Morales, L.; Wang, B.; Deffoe, T.; Takusagawa, F.; Mertes, M. P.; Mertes, K. B.; Paoletti, P. *Bioorg. Chem.* **1992,** *20,* 8−29.
(21) Papoyan, G.; Gu, K.; Wiórkiewicz-Kuczera, J.; Kuczera, K.; Bowman-James, K. *J. Am. Chem. Soc.* **1996**, *118*, 1354−1364.
(22) Mason, S.; Clifford, T.; Seib, L.; Kuczera, K.; Bowman-James, K. *J. Am. Chem. Soc.* **1998**, *120*, 8899−8890.

10.1021/ic9911116 CCC: $19.00
Published on Web 03/09/2000

Table 1. Crystallographic Data for $(H_6[26]aneN_6C_6)\cdot(6H_2PO_4^-)\cdot(2H_3PO_4)$

empirical formula	$C_{20}H_{52}N_6O_{32}P_8$
fw	1136.44
crystal system	monoclinic
space group	$P2_1/c$
a (Å)	10.0197(8)
b (Å)	12.5425(10)
c (Å)	19.235(2)
β (deg)	102.918(7)
V (Å^3)	2346.6(5)
Z	2
T (K)	296
λ (Å)	1.54178 (Cu Kα)
ρ_{calc} (g cm^{-3})	1.608
μ (cm^{-1})	37.4
crystal size (mm)	0.3 × 0.3 × 0.5
total reflns	3501
unique reflns	2917
reflns with $I > 2\sigma(I)$	2963
refined parameters	318
transmission factors	0.79−1.00
R [a]	0.040
R_w^2 [b]	0.1102
GOF	1.016
δF peak and hole (e$^-$ A^{-3})	0.702 and −0.339

[a] $R = ||F_o| - |F_c||/|F_o|$. [b] $R_w^2 = [w(F_o^2 - F_c^2)^2/wF_o^4]^{1/2}$ $w = 1/[\sigma^2(F_o^2) + (0.0566P)^2 + 2.8200P]$ where $P = (F_o^2 + 2F_c^2)/3$.

Further investigation indicated that this was a unique complex, containing both phosphoric acid and dihydrogen phosphate species, in addition to the macrocycle in the crystal structure. The crystal structures of dihydrogen phosphate and dihydrogen phosphate salts of acyclic polyamines have been published,[24,25] as well as two crystal structures of polyammonium macrocycles with pyrophosphate counterions.[26,27] To our knowledge, however, this is the first example of a crystal structure of a polyammonium macrocycle combined with either phosphoric acid or dihydrogen phosphate, not to mention both, in the same structure. Additionally, potentiometric studies indicate ditopic behavior for the macrocycle at low pHs, that is, the binding of two monohydrogen phosphates with one macrocycle.

Results and Discussion

Crystal Structure. The phosphoric acid/dihydrogen phosphate complex was obtained by reacting the macrocycle in the free-base form with phosphoric acid. Crystals suitable for X-ray analysis were obtained from recrystallization in methanol of the precipitate that was formed immediately after mixing. Crystallographic data are provided in Table 1.

In the crystal structure, the hexaprotonated macrocyclic cation is located on a crystallographic center of inversion and is surrounded by eight phosphate groups (Figure 1). Refined P−O distances (Table 2) and charge considerations indicate that the species involved are the cationic macrocycle, six dihydrogen phosphate anions ($H_2PO_4^-$), and two neutral phosphoric acid molecules (H_3PO_4). The situation is complicated by disorder in the crystal between the dihydrogen phosphate ions and the phosphoric acid molecules. This disorder is described in greater detail below.

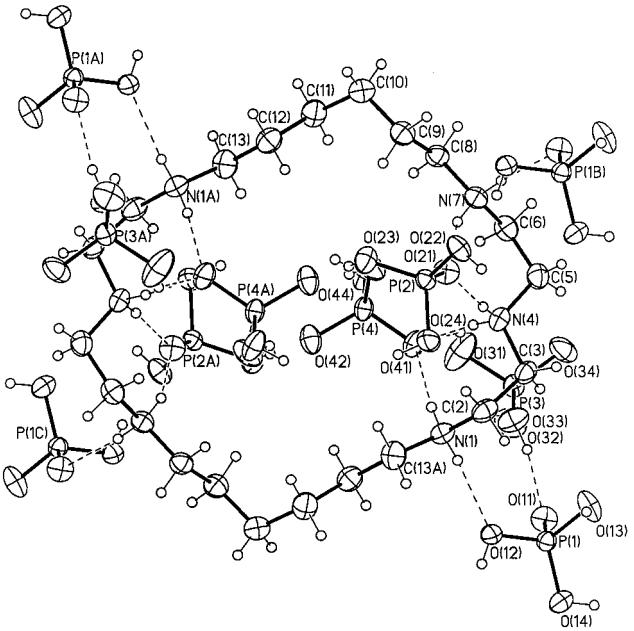

Figure 1. View of the cation and the four independent anions, with the inversion-related equivalents. Thermal ellipsoids are drawn at 50% probability.

Table 2. P−O Distances (Å) for $\{H_6[26]aneN_6C_6\}\cdot(6H_2PO_4)\cdot(2H_3PO_4)$

atoms	distance	atoms	distance
P(1)−O(11)	1.499(2)	P(3)−O(31)	1.542(3)
P(1)−O(12)	1.534(2)	P(3)−O(32)	1.499(2)
P(1)−O(13)	1.558(2)	P(3)−O(33)	1.558(2)
P(1)−O(14)	1.528(2)	P(3)−O(34)	1.496(2)
P(2)−O(21)	1.487(2)	P(4)−O(41)	1.506(2)
P(2)−O(22)	1.531(2)	P(4)−O(42)	1.505(2)
P(2)−O(23)	1.550(2)	P(4)−O(43)	1.565(2)
P(2)−O(24)	1.553(2)	P(4)−O(44)	1.552(2)

The macrocycle has the shape of a flat ellipsoid. The elliptical "major" axis runs between N(1) and N(1′), with a distance of 9.25 Å, whereas the "minor" axis length, C(8) to C(8′), is 8.361 Å. Torsion angles are shown in Table 3. The flattened shape of the macrocycle is achieved by consecutive *gauche* conformations of the same orientation at each "corner" of the macrocyclic ring and by *trans* conformations for the remaining sections. Interestingly, each of the three independent nitrogen atoms has a different orientation toward the ring to suit its bonding pattern, which consists of the formation of two strong hydrogen bonds ranging from 2.70 to 2.88 Å, with adjacent phosphates. N(1) points to the outside of the ring and therefore makes hydrogen bond contacts to phosphates 1 and 4; N(4) points toward the center of the macrocycle with hydrogen bonds to phosphates 2 and 4; and N(7) points upward from the macrocycle's mean plane and maintains hydrogen bonds with phosphates 1 and 2.

Assigning the types of phosphates in the crystal structure was not a straightforward matter because of the disorder between the two phosphate species. The hydrogen atoms on carbons and nitrogens were readily identifiable from difference Fourier maps. Pairs of long P−O bond distances in two of the four independent phosphate groups, P(3) and P(4) (Table 2), strongly indicated that these were dihydrogen phosphate anions, and their hydrogen atoms were also clear in the Fourier maps. However, P(1) and P(2) showed a spread of P−O distances, leaving it unclear which was the anion and which was the neutral species. After the inclusion of all but the final hydrogen atom, *two* relatively weak peaks appeared in acceptable locations, attached to O(11) and

(23) Wiórkiewicz-Kuczera, J.; Kuczera, K.; Bazzicalupi, C.; Bencini, A.; Valtancoli, B.; Bianchi, A.; Bowman-James, K. *New J. Chem.*, in press.
(24) Bartozak, E.; Jakolski, M. *Acta Crystallogr.* **1990**, *C46*, 2158−2160.
(25) Labadi, I.; Silanpaa, R.; Lonnberg, H. *J. Chem. Soc., Dalton Trans.* **1992**, 765−767.
(26) Lu, Q.; Motekaitis, R. J.; Reibenspies, J. J.; Martell, A. E. *Inorg. Chem.* **1995**, *34*, 4958−4964.
(27) Nation, D. A.; Reibenspies, J.; Martell, A. E. *Inorg. Chem.* **1996**, *35*, 4597−4603.

Table 3. Macrocycle Dihedral Angles (deg) for $\{H_6[26]N_6C_6\}\cdot(6H_2PO_4)\cdot(2H_3PO_4)$[a]

atoms	angle	atoms	angle
C(13′)−N(1)−C(2)−C(3)	−161.8(3)	C(6)−N(7)−C(8)−C(9)	171.3(3)
N(1)−C(2)−C(3)−N(4)	73.0(3)	N(7)−C(8)−C(9)−C(10)	−179.6(3)
C(2)−C(3)−N(4)−C(5)	174.2(3)	C(8)−C(9)−C(10)−C(11)	71.6(4)
C(3)−N(4)−C(5)−C(6)	168.8(3)	C(9)−C(10)−C(11)−C(12)	77.7(4)
N(4)−C(5)−C(6)−N(7)	67.5(3)	C(10)−C(11)−C(12)−C(13)	−176.9(3)
C(5)−C(6)−N(7)−C(8)	−170.0(3)	C(11)−C(12)−C(13)−N(1′)	−173.9(3)

[a] Primed atoms are related to unprimed atoms by $2 - x$, $1 - y$, $1 - z$.

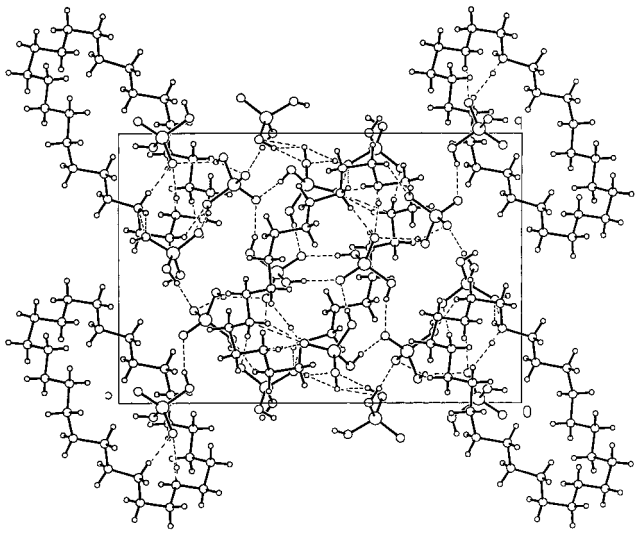

Figure 2. Packing diagram, viewed down *a*. Hydrogen atoms are omitted for clarity.

O(22), which make an unusually short contact. It was concluded that this proton is disordered between the two positions and that these phosphates make up a loosely bound $[H_3PO_4 - H_2PO_4]^-$ unit.

Key to the formation of the crystal structure is the intricate hydrogen-bond network involving the anionic and neutral phosphates and the cationic macrocycles. In addition to the hydrogen bonds linking the macrocycles to adjacent phosphates, a complex network of links between the phosphates runs through the structure. Phosphates P(2) and P(4) are located above and below the center of the macrocyclic cavity, whereas P(1) and P(3) are on each side of the ring. Phosphate P(1) is linked to four phosphates via symmetry-related occurrences of two phosphates (P(2) and P(3)), whereas each of the other phosphates is linked to three other phosphates. These hydrogen bonds produce a complete three-dimensional framework running through the crystal (Figure 2). Despite the disorder, the unusual occurrence of phosphoric acid in the crystal structure has been firmly established, not the least of which by the 1:8 macrocycle/phosphate stoichiometry. The result is a unique finding in this type of supramolecular complex.

Protonation Constants. To investigate the binding propensity of this ligand by potentiometric methods, the protonation constants for **1** were redetermined under the conditions used for binding studies (Table 4). Not only were they in close agreement with previous findings for this ligand with a different electrolyte concentration,[29] but they were also found to be similar to other ligands of the same family, such as [22]-aneN_6C_4[30] and [32]aneN_6C_9.[31] The first four constants are grouped and separated from the fifth by more than five logarithmic units, which is common with these hexaamine ligands. The pattern is readily rationalized, considering that an efficient minimization of electrostatic repulsion between positive charges in the tetraprotonated species is possible through the localization of the four acidic protons in alternating positions, separated by either the unprotonated nitrogen atoms or the aliphatic chain of six carbons. The much lower fifth and sixth protonation constants are due to the fact these last two protonations occur on the central nitrogens of each end of the macrocycle, and charge separation is no longer maximized.[28] The net effect of this pattern is that the major species present during the largest interval surrounding neutral pH, in effect pH 5−8, is the tetraprotonated species. The high degree of protonation at pHs surrounding physiological pH is one reason that this bis-triamine framework is so appealing for studies involving anions of biological relevance.

Table 4. (a) Stepwise Protonation Constants for ([26]aneN_6C_6)·(6 HCl) (L) and (b) Stepwise Binding Constants for the Interaction with Phosphate and Protonated Phosphate Species in 0.1 mol dm^{-3} NaCl at 298.1 ± 0.1 K

reaction	log *K*
(a) Stepwise Protonation Constants	
$H^+ + L = HL^+$	10.94(4)[a]
$HL^+ + H^+ = H_2L^{2+}$	9.81(2)
$H_2L^{2+} + H^+ = H_3L^{3+}$	9.59(4)
$H_3L^{3+} + H^+ = H_4L^{4+}$	9.14(3)
$H_4L^{4+} + H^+ = H_5L^{5+}$	3.75(3)
$H_5L^{5+} + H^+ = H_6L^{6+}$	3.07(3)
(b) Stepwise Binding Constants	
$H_3L^{3+} + P^{3-} = H_3LP$	4.55(4)[b]
$H_3L^{3+} + HP^{2-} = H_4LP^+$	2.23(8)
$H_4L^{4+} + HP^{2-} = H_5LP^{2+}$	2.49(6)
$H_5L^{5+} + HP^{2-} = H_6LP^{3+}$	6.01(3)
$H_5L^{5+} + 2H_2P^- = H_9LP_2{}^{3+}$	6.16(6)
$H_6L^{6+} + 2H_2P^- = H_{10}LP_2{}^{4+}$	6.44(5)

[a] Values in parentheses are the standard deviations in the last significant digit.

Unlike some other simple mononegative anions, such as the halides, nitrate, and perchlorate, binding studies involving phosphate present a more complex scenario. This is due to the four possible forms that occur in varying amounts, depending on pH, from PO_4^{3-} at high pH, through the mono- and dianions, to the fully protonated neutral H_3PO_4, the latter found at very low pH. For the purposes of this study, the distribution diagram for the phosphate species was also redetermined under the same conditions used for binding studies. At pH ∼7, the situation is complicated by the presence of both the mono- and diprotonated forms of phosphate in almost equal quantities.

Binding Constants. The binding constants were determined for the interaction of [26]aneN_6C_6, **1**, with phosphate (Table 4 and Figure 3). Starting at the highest pHs, the triprotonated form of the macrocycle appears to form a fairly stable neutral complex with the trinegatively charged phosphate ion $[H_3LP]$, as might

(28) Bencini, A.; Bianchi, A.; García-España, E.; Micheloni, M.; Ramírez, J. A. *Coord. Chem. Rev.* **1999**, *188*, 97−156.
(29) Cruise, R. W.; Kaderli, S.; Spieler, W.; Zuberbuhler, A. D. *Helv. Chim. Acta* **1988**, *71*, 562−568.
(30) Hosseini, M. W.; Lehn, J.-M. *Helv. Chim. Acta* **1986**, *69*, 587−603.
(31) Martin, A. E.; Bulkowskii, J. E. *J. Org. Chem.* **1982**, *47*, 415−418.

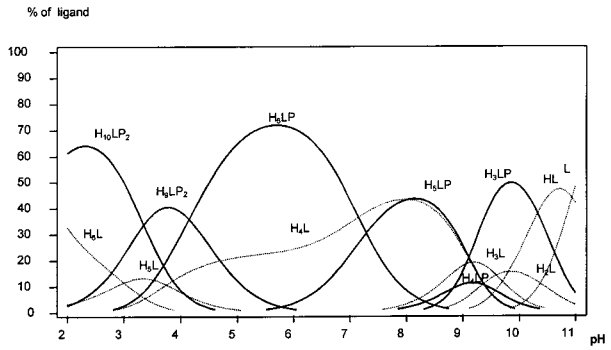

Figure 3. Distribution diagrams of the species for the system [26]-aneN$_6$C$_6$ (L) and PO_4^{3-} (P) in 0.1 mol dm^{-3} NaCl at 298.1 ± 0.1 K as a function of pH. ([L] = 1×10^{-3} mol dm^{-3}, [P] = 2×10^{-3} mol dm^{-3}).

be anticipated from the charge "complementarity" (log K_{as} = 4.55(4)), where P = PO_4^{3-} and L = **1** in its neutral form. The lower observed binding for the next constant, that is, the formation of the $[H_4LP]^+$ species, can be attributed to binding with the monoprotonated HPO_4^{2-}, which, in the absence of other species, maximizes around pH 9. Hence, this species is more appropriately written as $[H_3LHP]^+$, and as expected, the affinity decreases with the decreased charge on the anion. The next two constants also probably involve binding of predominantly the monoprotonated HPO_4^{2-} species. The affinity increases significantly once the macrocycle becomes pentaprotonated. The major complex observed during the widest range of pH is $[H_6LP]^{3+}$ (mostly due to the $[H_5LHP]^{3+}$species), log K_{as} = 6.01(3). In fact, at a pH slightly less than 6, approximately 70% of the receptor can be considered as being complexed.

Because of the geometry of this ligand, with two triamine subunits held together by two aliphatic chains, the potential of ditopic behavior can be envisioned. Potentiometric evidence for ditopic binding in instances involving ammonium-based monocyclic receptors with anions has not previously been reported to our knowledge. Here, however, in keeping with the crystallographic results, potentiometric data indicate the binuclear ternary complexes $[H_9LP_2]^{3+}$ (predominantly $[H_5L{\cdot}2H_2P]^{3+}$) and $[H_{10}LP_2]^{4+}$ (predominantly $[H_6L{\cdot}2H_2P]^{4+}$), which are products of the binding of pentaprotonated and hexaprotonated forms of the ligand with two molecules of $H_2PO_4^-$ at pHs between 2 and 4. These findings can be correlated with the crystal structure and strong hydrogen bonding interactions between the macrocycle and the two ordered $H_2PO_4^-$ species, (P(4) and P(4A)), which are almost inside the macrocyclic ring.

Conclusions

The structural and binding results for the interaction of the hexaprotonated ligand **1** with phosphate show some very interesting trends. Potentiometric data indicate that initial binding occurs at even relatively high pH, with the formation of a stable neutral $[H_3LP]$ complex. The crystal structure, on the other hand, essentially provides a snapshot of the situation occurring at relatively low pH, in which both $H_2PO_4^-$ and H_3PO_4 are present. This is an unusual, if not unprecedented, crystallographic documentation of both $H_2PO_4^-$ and H_3PO_4 together in a supramolecular complex. Furthermore, the potentiometric data support the crystallographic finding of two $H_2PO_4^-$ species closely associated with the macrocycle and give credence to the supposition that these types of ligands, based on two triamine units, can provide ditopic binding sites for two discrete anions.

Experimental Section

Synthesis. All chemicals were reagent grade or better. The receptor 1,4,7,14,17,20-hexaazacyclohexacosane, [26]N$_6$C$_6$ (**1**), was synthesized according to a modified procedure of previously published preparations.[31] A precipitate immediately formed upon reacting the macrocycle in the free-base form with phosphoric acid in approximately a 1:6 macrocycle/phosphoric acid ratio. The precipitate was filtered under nitrogen, and the residue was redissolved in 400 μL of aqueous methanol. A limited number of crystals suitable for X-ray analysis were obtained by the slow evaporation of the latter solution in a capillary tube.

X-ray Structural Analysis. Crystallographic data for **1**·6H_2PO_4·2H_3PO_4 are summarized in Table 1. Data were collected on a Rigaku AFC5R diffractometer with a 12 kW rotating anode generator using graphite-monochromated Cu Kα radiation. The data were collected using the $\omega-2\theta$ scan technique to a maximum 2θ value of 110.2°, with stationary background counts recorded on each side of the reflection. The ratio of peak counting time to background counting time was 2:1. The weak reflections were rescanned (maximum of two rescans), and the counts were accumulated. The intensities of three representative reflections were measured every 150 scans and remained essentially constant throughout data collection, so no correction for decay was deemed necessary. The data were corrected for Lorentz and polarization effects. An empirical absorption correction[32] was made based on azimuthal scans of several reflections and resulted in transmission factors ranging from 0.79 to 1.00.

The structure was solved by direct methods[33] and all of the non-hydrogen atoms were refined anisotropically. The final cycle of full-matrix least-squares refinement was based on the 2917 observed reflections ($I > 0.01\sigma(I)$) and 402 variable parameters and converged (largest parameter shift was 0.01 times its esd). The weighting scheme, based on counting statistics, included a factor, $p = 0.05$, to downweight the intense reflections. Neutral atom scattering factors were taken from Cromer and Waber.[34] Anomalous dispersion effects were included in F_{calc}.[35] The values for $\Delta f'$ and $\Delta f''$ were those of Cromer.[36] All of the calculations were performed using the teXsan crystallographic software package of the Molecular Structure Corp.[37] Listings of the final positional coordinates and isotropic temperature factors are provided in Table 2.

Potentiometric Measurements. The potentiometric titrations were carried out in 0.1 mol dm^{-3} NaCl at 298.1 ± 0.1 K. Emf data were obtained using an Orion 81−02 combination electrode with 1 M potassium tosylate filling solution. The electrode was calibrated as a hydrogen-ion concentration probe by the titration of known amounts of HCl with CO_2-free NaOH solutions. The equivalence point was determined by Gran's method, which gives the standard potential ($E^{\circ\prime}$) and the ionic product of the water (pK_w = 13.79). The concentration of the phosphate solution employed was determined gravimetrically by standard methods.

The computer program SUPERQUAD[38] was used to calculate the protonation and stability constants, and the program DISPO[39] was used to obtain the distribution diagrams. The titration curves for each system

(32) Walker, N. P. C.; Stuart, D. I. *Acta Crystallogr*. **1983**, *A39*, 158−166.
(33) Direct methods used were MITHRIL (Gilmore, C. J. *J. Appl. Crystallogr*. **1984**, *17*, 42) and DIRDIF: Beurskens, P. T. Technical Report Crystallography Laboratory, Toernooiveld, 6525 E. Nijmegen, The Netherlands, 1985.
(34) Cromer, D. T.; Waber, J. T. In *International Tables for X-ray Crystallography*; Kynoch Press: Birmingham, 1974; Vol. 4, Table 2.2A.
(35) Ibers, J. A.; Hamilton, W. C. *Acta Crystallogr*. **1964**, *17*, 781−782.
(36) Cromer, D. T. In *International Tables for X-ray Crystallography*; Kynoch Press: Birmingham, 1974; Vol. 4, Table 2.3.1.
(37) TEXSAN-TEXRAY Structure Analysis Package; Molecular Structure Corp.: 1985.
(38) Gans, P.; Sabatini, A.; Vacca, A. *J. Chem. Soc., Dalton Trans* **1985**, 1195.
(39) Vacca, A. Unpublished work: a FORTRAN program to determine the distribution of the species in multi-equilibria systems from the stability constants and mass balance equations.

corresponded to 150 experimental points obtained by at least three measurements taken along the pH range investigated (2−11). The concentrations of both receptor and phosphate were 1×10^{-3} to 3×10^{-3} mol dm^{-3}. The data were treated either as a single set or as separated curves without significant variations in the values of the stability constants. All of the sets of data were merged to give the final stability constants. The protonation constants of PO_4^{3-} were also redetermined under the same experimental conditions.[40]

(40) Basicity constants for phosphate in 0.1 M NaCl at 287.1 ± 0.1 K: log β_1 = 11.15(1), log β_2 = 17.85(1), log β_3 = 19.99(2).

Acknowledgment. This work was supported by a grant from the Department of Energy, Grant No. DE-FG07-96ER62307. The help of Larry Seib in the X-ray Crystallography Laboratory at the University of Kansas is greatly appreciated.

Supporting Information Available: Figures consisting of a side view of the macrocycle and distribution diagrams of [26]aneN_6C_6 and phosphate. One X-ray crystallographic file in CIF format is available. This material is available free of charge via the Internet at http://pubs.acs.org.

IC9911116